Uludağ University Journal of The Faculty of Engineering, Vol. 31, No. 2, 2026 RESEARCH

DOI: 10.17482/uumfd.1621689

DUAL-BAND DRONE GPS ANTENNA DESIGN AND APPLICATION

Alperen TOKDEMİR [*]
Begüm KARAIŞIK [*]
Ediz ERDEM [*]

Received: 16.01.2025; revised: 25.02.2026; accepted: 20.04.2026

Abstract: This study investigates the design and development of a dual-band directional microstrip patch antenna for unmanned aerial vehicles (UAVs). The antenna is optimized to operate within the GPS L_1 (1.57 GHz) and L_2 (1.22 GHz) frequency bands. It is designed to enhance long-distance transmission performance by optimizing gain and directivity, particularly for UAV communication. The primary objective of this study is to develop a cost-effective, locally developed antenna solution suitable for counter-UAV applications in controlled and authorized environments. The antenna design was simulated using CST Studio and validated through experimental testing. The simulation and experimental measurements demonstrated excellent impedance matching and efficient performance across both frequency bands. The antenna pattern was precisely etched onto the FR-4 substrate during manufacturing using photolithographic techniques. The proposed structure offers a compact, lightweight, and low-cost solution suitable for integration into small- and medium-sized UAV platforms.

Keywords: UAVs, Antenna design, GPS, Dual-Band

Çift Bantli İHA Küresel Konumlandirma Sistemi Anten Tasarimi ve Uygulaması

Öz: Bu çalışma, insansız hava araçları (İHA) için çift bantlı yönlü mikro şerit yama anteninin tasarımı ve geliştirilmesi araştırmaktadır. Anten, GPS sisteminin L_1 (1.57 GHz) ve L_2 (1.22 GHz) frekans bantlarında çalışacak şekilde optimize edilmiştir. Özellikle insansız hava aracı iletişimi için kazancı ve yönlülüğü optimize ederek uzun mesafeli iletim performansını artırmak üzere tasarlanmıştır. Bu çalışmanın temel amacı, kontrollü ve yetkili ortamlarda insansız hava araçlarına karşı uygulamalar için uygun, maliyet etkin ve yerel olarak geliştirilmiş bir anten çözümü geliştirmektir. Anten tasarımı CST Studio kullanılarak simüle edilmiş ve deneysel testlerle doğrulanmıştır. Simülasyon ve deneysel ölçümleri, her iki frekans bandında da mükemmel empedans uyumu ve verimli performans göstermiştir. Anten deseni, fotolitografik teknikler kullanılarak üretim sırasında FR-4 alt tabaka üzerine hassas bir şekilde işlenmiştir. Önerilen yapı, küçük ve orta ölçekli İHA platformlarına entegrasyon için uygun, kompakt, hafif ve düşük maliyetli bir çözüm sunmaktadır.

Anahtar Kelimeler: İHA, Anten Tasarımı, Küresel Konumlandırma Sistemi, Çift Bant

1. INTRODUCTION

UAVs have become increasingly significant in modern communication and navigation systems due to their expanding roles in civil, commercial, and defense-related applications (Ahmed et al., 2025; Brown, 2023). Initially developed for military purposes, UAV technologies are now widely used in infrastructure inspection, environmental monitoring, precision agriculture, aerial imaging, logistics, and surveillance operations (Arpaio et al., 2021). Their ability to perform

[*] Department of Electrical and Electronics Engineering, Karabuk University, 78050, Karabuk, Türkiye
Corresponding Author: edizerdem@karabuk.edu.tr

tasks in hazardous or inaccessible environments provides substantial operational flexibility and cost efficiency.

The rapid growth of UAV platforms has been accompanied by increased integration into space–air–ground communication networks, enabling reliable connectivity between airborne systems and terrestrial or satellite infrastructures (Chen et al., 2025). This evolution requires lightweight, compact, and aerodynamically efficient antenna systems capable of maintaining stable communication and navigation performance. Since UAV flight duration is constrained by battery capacity, antenna designs must minimize size and weight while preserving adequate gain and radiation characteristics. Furthermore, the growing demand for multi-frequency operation and robust positioning performance has increased interest in dual-band and multiband antenna structures (Zhu et al., 2024).

Microstrip patch antennas are widely preferred in UAV platforms due to their low profile, mechanical robustness, low fabrication cost, and ease of integration with planar circuits (Zaki & Rahman, 2025). These antennas typically consist of a metallic radiating patch printed on a dielectric substrate, with a ground plane backing (Irıqat & Yenikaya, 2024). Their resonant frequency, bandwidth, gain, and radiation characteristics can be tailored through geometrical modifications and material selection. However, conventional microstrip antennas inherently exhibit relatively narrow bandwidth and moderate gain, often necessitating structural enhancements for demanding wireless applications (Balanis, 2016).

UAV positioning and navigation are predominantly supported by the Global Positioning System (GPS), which operates in the L_1 (1.57 GHz) and L_2 (1.22 GHz) frequency bands (Erbaş, 2023; Kaplan & Hegarty, 2017). Modern UAV systems may also integrate additional Global Navigation Satellite Systems (GNSS), such as GLONASS, Galileo, and BeiDou, to improve positioning reliability and accuracy. As UAV usage expands in urban and sensitive environments, the need for reliable signal acquisition, interference resilience, and controlled spectrum management has become increasingly important (Natgunanathan et al., 2023).

Recent research has therefore focused on enhancing antenna performance parameters such as gain, directivity, bandwidth, and multi-band capability for UAV-related applications (S et al., 2025). Various approaches, including slot loading, stacked patches, parasitic elements, and metamaterial-inspired structures, have been proposed to achieve dual-band operation while maintaining compact geometry (Chen et al., 2025; Ha et al., 2024). Dual-band GPS antennas are particularly relevant for UAV systems because simultaneous access to L_1 and L_2 bands improves positioning robustness and operational flexibility.

In this study, a compact dual-band directional microstrip patch antenna operating at GPS L_1 (1.57 GHz) and L_2 (1.22 GHz) bands is proposed. Unlike many dual-band designs that require multilayer or stacked configurations, the proposed structure employs symmetrically positioned I-shaped slots on a single-layer FR-4 substrate to achieve dual-band resonance. This approach maintains structural simplicity, low fabrication cost, and ease of practical implementation while providing adequate electromagnetic performance. The antenna design is validated through full-wave simulations and experimental measurements, demonstrating its suitability for integration into UAV-based communication and navigation systems and for controlled counter-UAV applications within authorized operational frameworks.

2. MATERIALS AND METHODS

A microstrip antenna typically comprises a radiating patch on one side of a dielectric substrate and a ground plane on the other (Karacoban et al., 2022). This planar structure, consisting of a patch, a substrate, and a ground plane, offers advantages such as a low profile, ease of fabrication, and compatibility with integrated circuits. The electromagnetic performance of a microstrip antenna, specifically its operating frequency, gain, bandwidth, directivity, and polarization, is significantly influenced by the material properties, geometrical dimensions, and configuration of these constituent layers (Balanis, 2016).

The design process involves carefully optimizing key parameters to meet targeted performance specifications. Critical factors such as patch dimensions, substrate type, and dielectric constant are adjusted to achieve the desired frequency range, impedance matching, and radiation characteristics. Through such optimization, microstrip antennas can be customized for specific applications in modern communication systems (Kodheli et al., 2020; Sorgucu, 2024).

In this study, the antenna was designed to operate within the 1.22–1.57 GHz frequency range. The dielectric substrate is placed between the radiating patch and the ground plane, and its dielectric constant plays a crucial role in determining the antenna's dimensions and performance. As the dielectric constant increases, the antenna's physical size decreases; however, lower dielectric constants generally yield better efficiency and broader bandwidth. The fringing fields at the patch edges also increase the antenna's effective electrical length. Increasing the substrate thickness, provided surface wave propagation is minimized, can improve radiation efficiency by up to 90% and bandwidth by up to 35%. Nevertheless, excessive substrate thickness can lead to undesirable surface-wave excitation, reducing radiation efficiency and distorting the radiation pattern due to scattering at discontinuities, such as the dielectric corners (Balanis, 2016).

Although GPS signals are typically right-hand circularly polarized (RHCP), the antenna proposed in this study is linearly polarized. To ensure fabrication simplicity and cost-effectiveness, a linear polarization approach was adopted. Circular polarization was not implemented in the current design phase; however, future iterations may explore techniques such as truncated corners or dual-feed structures to enable circular polarization.

In antenna design, patch width W_p and length L_p must be analytically determined. Here, ε_r and λ_0 are the relative permittivity of the substrate and the wavelength in free space at the operating frequency, respectively. The optimal choice of w_p ensures excellent impedance matching (Ahmad et al., 2021) and is given (1).

$$W_P = \frac{\lambda_0}{2\left(\sqrt{0.5(\varepsilon_r+1)}\right)} \tag{1}$$

The length of the patch can be evaluated using Equation (2):

$$L_P = \frac{c_0}{2fo\sqrt{\varepsilon_{eff}}} - 2\Delta L_p \tag{2}$$

Here, c_0 is the speed of light; ΔL is the change in the patch length due to the fringing effect; and ε_{eff} is the effective dielectric constant. The effective relative permittivity can be calculated using Equation (3)

$$\varepsilon_{eff} = \frac{\varepsilon_r+1}{2} + \frac{\varepsilon_r-1}{2}\left(\frac{1}{\sqrt{1+12\frac{h_s}{w_p}}}\right) \tag{3}$$

Here, h_s is the substrate height. Finally, the fringing effect can be calculated using Equation (4):

$$\Delta L_p = 0.421 h_s \frac{\left(\varepsilon_{eff}+0.300\right)\left(w_p/h_s+0.264\right)}{\left(\varepsilon_{eff}-0.258\right)\left(W_p/h_s+0.813\right)} \tag{4}$$

2.1. Design of Antenna

The patch dimensions of the antenna decrease as the frequency increases. First, the width and length of the patch section of the antenna to be designed were calculated using formulas 1-4, operating at a frequency of 1.22 GHz. For the dielectric layer, a 1.6 mm thick, widely available, and affordable FR-4 material with a dielectric constant of 4.3 was used. The widths and lengths are the primary line dimensions of the antenna. Dual-band operation at L_1 and L_2 was achieved by incorporating I-shaped slots into the patch geometry. The main antenna comprises a simple 50-Ω feedline, a rectangular patch, and a ground plane. The geometric structure and basic components of the designed antenna are shown in Figure 1. The I-shaped slots enable dual-band operation at GPS L_1 (1.57 GHz) and L_2 (1.22 GHz) frequencies.

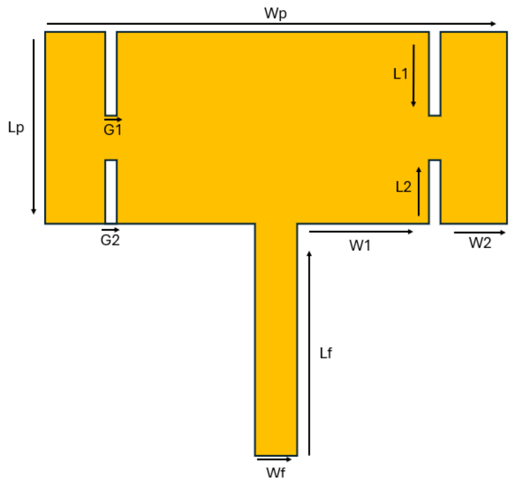

Figure 1:
The I-shaped slots are placed on both upper and lower sides of the patch to enable dual-band operation

A high-performance 3D electromagnetic analysis software, CST (Computer Simulation Technology), was used to design and optimize the directional patch GPS antenna. The optimization process was carried out to add slots and create two bands. In the first step, I-shaped slots were introduced on the upper section of the radiating patch to shift the antenna's lower frequency band from 1.1 GHz to 1.22 GHz. These slots adjust the antenna's resonant frequency and bandwidth. In the second step, I-shaped slots are added to the lower side of the radiation patch to enable the antenna to operate in two frequency bands (1.22 GHz and 1.57 GHz). These slots are carefully sized to optimize the antenna's bandwidth and impedance matching (Tütüncü et al., 2022). The designed antenna parameter values are given in Table 1.

Table 1. Antenna design parameters

Parameters	Values (mm)	Parameters	Values (mm)
W_p	64.8	L_p	57.6
L_1	25.8	L_2	19.2
L_f	24.9	G_1	1.3
H_s	1.6	G_2	1.4
H_g	0.035	H_p	0.035
W_1	21.9	W_2	8
W_f	2.2		

2.2. Fabrication

The proposed dual-band directional microstrip patch antenna was fabricated using an FR-4 substrate and copper as the radiating material. The FR-4 substrate, selected for its widespread availability, cost-effectiveness, and suitable dielectric properties (dielectric constant $\varepsilon_r = 4.3$), has a thickness of 1.6 mm. A standard copper cladding with a thickness of 0.035 mm was used for both the patch and the ground plane.

The antenna dimensions were determined through analytical calculations and simulation-based optimization, resulting in a compact structure measuring 64.8 mm × 57.6 mm × 1.6 mm. The fabricated antenna weighs 28 grams, making it well-suited for integration into small- and medium-sized UAV platforms without significantly affecting flight dynamics or payload capacity. Its low profile and planar geometry help minimize aerodynamic drag, an essential consideration in UAV design.

The fabrication process began by cutting the FR-4 substrate to the specified dimensions. The antenna pattern, including the rectangular patch, feed line, and I-shaped slots, was transferred onto the copper layer using standard photolithographic techniques. This involved coating the copper surface with a UV-sensitive photoresist, exposing it through a patterned mask, and developing the image to define the desired geometry. Subsequent chemical etching removed the unprotected copper, yielding a precise antenna layout.

Following etching, the substrate was cleaned, and the antenna underwent visual inspection and preliminary continuity testing. The final prototype was subjected to electrical performance measurements to verify impedance matching and dual-band operation. The front side (a) presents the etched patch and slots, while the back side (b) shows the continuous ground plane, as shown in Figure 2.

Figure 2:

Fabricated dual-band patch antenna;
***a.** Front view showing the patch and feed line **b.** Back view showing the ground plane*

2.3. Measurement Setup

The setup includes the antenna under the test connected via a coaxial cable to a calibrated vector network analyzer, as shown in Figure 3. The configuration measured S-parameters (particularly S_{11}) across the target GPS frequency bands. Thru-reflect-line calibration (Delihasanlar & Yuzer, 2017; Erdem & Yuzer, 2022) was performed to prevent errors in the measurement setup. After the measurement, antenna parameters were calculated using the S-parameters taken from the network analyzer.

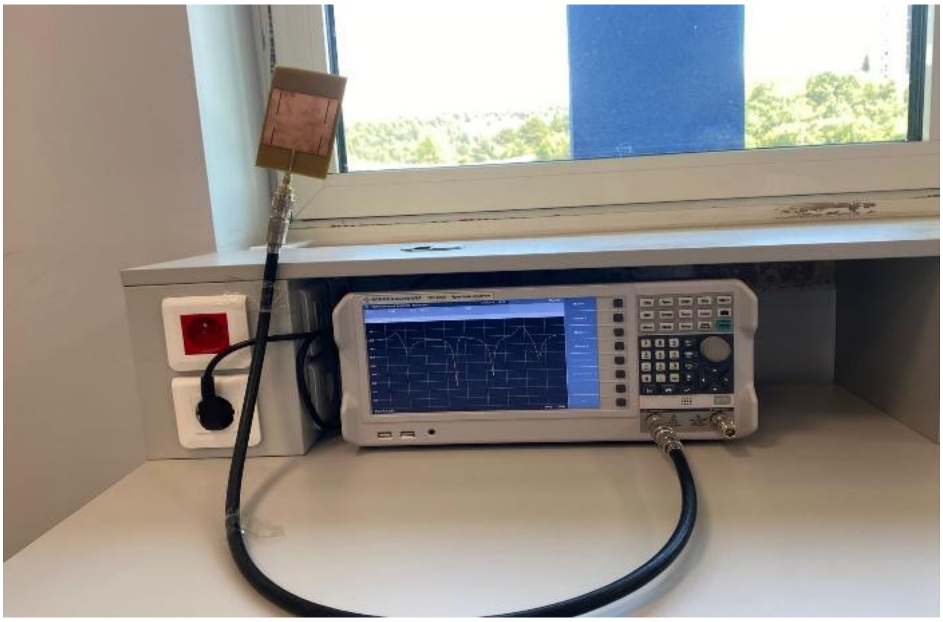

Figure 3:
Measurement setup using a vector network analyzer

3. RESULTS AND DISCUSSIONS

The simulated far-field directivity patterns of the designed antenna in free space at 1.22 GHz and 1.57 GHz are shown in Figures 4 and 5, respectively.

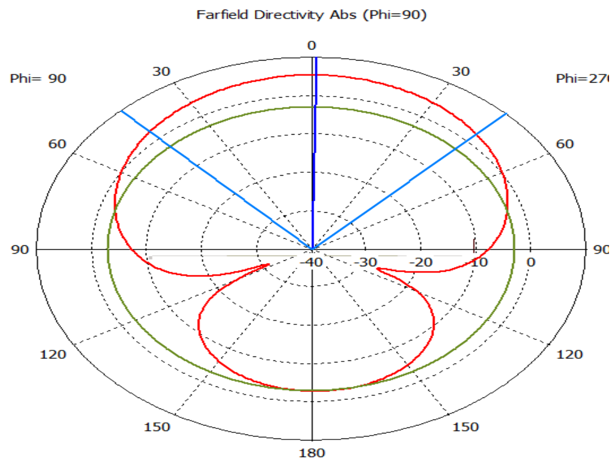

Figure 4:
Directivity pattern of 1.22 GHz

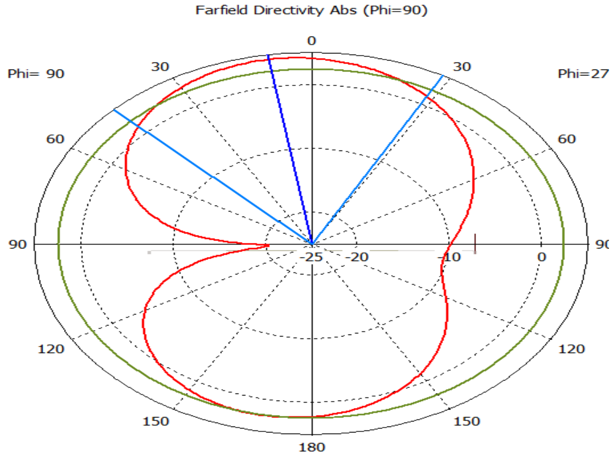

Figure 5:

Directivity pattern of 1.57 GHz

At 1.22 GHz, the main lobe is centered around 1°, with a peak directivity of 5.35 dBi, indicating strong radiation in the forward direction. The side lobes are relatively suppressed, with a side lobe level of -8.3 dB, which is favorable for minimizing interference from undesired directions. At 1.57 GHz, the main lobe shifts slightly to 9°, with a directivity of 4.25 dBi. The higher side lobe level at this frequency, -1.9 dB, suggests more distributed radiation, possibly due to increased coupling effects from the slots. The radiation patterns at both frequencies confirm the antenna's effectiveness in focusing energy in specific directions, which is advantageous for directional UAV communication or controlled counter-UAV applications. The asymmetry in the lobe shapes between the two frequencies reflects the antenna's dual-band behavior through the slot structure that supports operation at both L_1 and L_2 bands. The far-field parameters of the designed antenna in free space at 1.22 GHz and 1.57 GHz are given in Table 2.

Table 2. Far-fields parameters

Parameters	1.22 GHz	1.57 GHz
Directivity	5.348 dBi	4.245 dBi
Main Lobe Magnitude	5.35 dBi	4.25 dBi
Main Lobe direction	1.0 deg.	9.0 deg.
Side Lobe Level	-8.3 dB	-1.9 dB

The comparison between the simulated and measured S_{11} parameters of the antenna is illustrated in Figure 6.

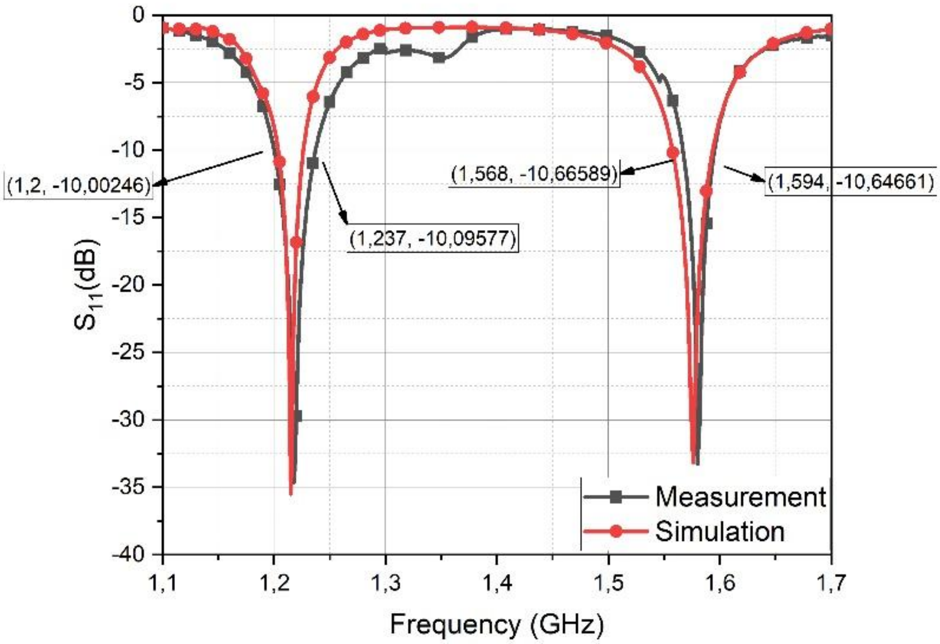

Figure 6:
Simulation and measurement S_{11} results

At the lower frequency band, 1.22 GHz, the simulated and measured S_{11} values are approximately -36 dB and -30 dB, respectively. At the higher frequency band, 1.57 GHz, the simulation indicates an S_{11} value reaching approximately -32 dB, whereas the measured value is about -28 dB. A bandwidth of 260 MHz was achieved in the L_1 band and 370 MHz in the L_2 band. The slight discrepancy between simulation and measurement can be attributed to potential practical factors such as fabrication tolerances, material properties, and measurement environment inconsistencies. The antenna exhibits good impedance matching at both targeted frequencies of 1.22 GHz and 1.57 GHz. The results confirm its suitability for practical implementations within these frequency bands.

4. CONCLUSION

This study presented the design and development of a dual-band directional microstrip patch antenna optimized for GPS L_1 (1.57 GHz) and L_2 (1.22 GHz) frequency bands. Fabricated on an FR-4 substrate with copper radiating elements, the proposed antenna achieved impedance matching and directional gain. System-level evaluations demonstrated that the antenna's lightweight design (28 g), compact dimensions (64.8 mm × 57.6 mm × 1.6 mm), and passive operation make it suitable for integration into small- to medium-sized unmanned aerial vehicles (UAVs), particularly for applications such as surveillance, navigation, and counter-UAV systems.

A key contribution of this work is the introduction of a novel single-layer dual-band antenna that uses I-shaped slots to enable simultaneous L_1 and L_2 GPS operation. This design prioritizes simplicity, manufacturability, and practical implementation without compromising performance. The antenna's planar structure facilitates seamless installation on UAV platforms with minimal aerodynamic interference.

Although in-flight validation was beyond the scope of the current study, the antenna's physical and electromagnetic characteristics, such as high directivity and low profile, suggest potential suitability for in-flight operation. Future work will focus on real-time testing in operational UAV scenarios, including aerodynamic performance assessments and environmental resilience under dynamic flight conditions.

ACKNOWLEDGEMENTS

Research Fund of the Karabuk University supported this work. Project Number: KBÜBAP-24-DS-133

CONFLICT OF INTEREST

The authors confirm that they have no conflicts of interest or shared interests with any institution, organization, or individual.

AUTHOR CONTRIBUTION

Alper Tokdemir contributes to determining the conceptual, design, and fabrication processes and conducting data analysis and interpretation. Begum Karaisik contributes to deciding the conducting data analysis and interpretation and writing the original draft. Ediz Erdem contributes by managing conceptual design and fabrication processes and reviewing, editing, and supervising.

REFERENCES

1. Ahmad, S., Ghaffar, A., Hussain, N., & Kim, N. (2021). Compact dual-band antenna with paired l-shape slots for on-and off-body wireless communication. *Sensors*, *21*(23). https://doi.org/10.3390/s21237953

2. Ahmed, W. A., Alage, L., Mala, B., & Olatoyinbo, S. F. (2025). Evolution of GNSS / GPS technology and its applications from ancient times to the present. *Next Research*, *2*(3), 100387. https://doi.org/10.1016/j.nexres.2025.100387

3. Arpaio, M. J., Paolini, G., Fuschini, F., Costanzo, A., & Masotti, D. (2021). An all-in-one dual band blade antenna for ads-b and 5g communications in uav assisted wireless networks. *Sensors*, *21*(17). https://doi.org/10.3390/s21175734

4. Balanis, C. A. (2016). *Antenna theory: analysis and design*. John wiley & sons.

5. Brown, A. D. (2023). Radar challenges, current solutions, and future advancements for the counter unmanned aerial systems mission. *IEEE Aerospace and Electronic Systems Magazine*, *38*(9), 34–50.

6. Chen, Z. et al. (2025). Low-Profile All-Metal Dual-Band Dual-Polarized Shared-Aperture Phased Arrays for UAV Applications. *IEEE Internet of Things Journal*, *PP*, 1. https://doi.org/10.1109/JIOT.2025.3573990

7. Delihasanlar, E., & Yuzer, A. H. (2017). Simulation modelling and calculation of dielectric permittivity of Opuntia at 1.7–2.6 GHz. *Journal of Microwave Power and Electromagnetic Energy*, *51*(2), 150–158. https://doi.org/10.1080/08327823.2017.1321463

8. Erbaş, C. D. (2023). Dual-band and dual-mode annular ring microstrip patch antenna with slots for GSM-1800 and GPS operations. *Journal of the Faculty of Engineering and Architecture of Gazi University*, *38*(1), 547–556. https://doi.org/10.17341/gazimmfd.740475

9. Erdem, E., & Yuzer, A. H. (2022). Textile-based 3D metamaterial absorber design for X-band application. *Waves in Random and Complex Media*. https://doi.org/10.1080/17455030.2022.2144655

10. Ha, N., Kim, G., Bae, H. C., & Kim, S. (2024). Compact Dual-Band, Dual-Circular Polarized Microstrip Antenna Array for K/Ka-Band Application. *IEEE Open Journal of Antennas and Propagation*, *6*(2), 372–382. https://doi.org/10.1109/OJAP.2024.3518556

11. Irıqat, S., & Yenikaya, S. (2024). Microstrip Patch Antenna Design With Enhanced Radiation Efficiency for 5G 60 Ghz Millimeter-Wave Systems. *Uludağ University Journal of The Faculty of Engineering*, *29*(1), 101–112. https://doi.org/10.17482/uumfd.1366173

12. Kaplan, E. D., & Hegarty, C. (2017). *Understanding GPS/GNSS: principles and applications*. Artech house.

13. Karacoban, G., Gokkaya, M. N., & Erdem, E. (2022). Logo Antenna Design and Application for 5G Applications. In *1st International Conference on Scientific and Academic Research* (pp. 400–402).

14. Kodheli, O. et al. (2020). Satellite communications in the new space era: A survey and future challenges. *IEEE Communications Surveys & Tutorials*, *23*(1), 70–109.

15. Natgunanathan, I., Fernando, N., Loke, S. W., & Weerasuriya, C. (2023). Bluetooth low energy mesh: Applications, considerations and current state-of-the-art. *Sensors*, *23*(4), 1826.

16. S, A. K., V K, S., B, T., S, M., S, J. A., K, K., & S, S. (2025). Antennas in Unmanned Aerial Vehicles - A Short Review. In *2025 3rd International Conference on Advancements in Electrical, Electronics, Communication, Computing and Automation (ICAECA)* (pp. 1–5). IEEE. https://doi.org/10.1109/ICAECA63854.2025.11012308

17. Sorgucu, U. (2024). Potential of Commercial Titanium in Electromagnetic Shielding for 5G Frequency Domain TT - 5G Frekans Bölgesi için Ticari Titanyumun Elektromanyetik Ekranlama Potansiyeli. *Mühendislik Bilimleri ve Araştırmaları Dergisi*, *6*(2), 198–207. https://doi.org/10.46387/bjesr.1511306

18. Tütüncü, B., Altintaş, Y., & Karahan, S. (2022). High-Efficiency Dual Band Metamaterial Absorber For ISM Band Biosensor Applications. In *2022 International Congress on Human-Computer Interaction, Optimization and Robotic Applications (HORA)* (pp. 1–3). IEEE.

19. Zaki, M., & Rahman, A. (2025). Innovations in Microstrip Antenna Design for IOT : Efficiency , Miniaturization , and Production Costs. *Journal of Engineering, Technology and Social Science*, *11*(1), 27–40.

20. Zhu, T., Xiao, B., & Wang, Z. (2024). Dual-Band SIW Antenna with High Frequency Ratio for UAV Detection Applications. *IETE Journal of Research*, *2063*. https://doi.org/10.1080/03772063.2024.2399146